Hamida, Z. and Goulet, J-A. (Preprint 2021). *Quantifying the Effects of Interventions Based on Visual Inspections from a Network of Bridges.* Structure and Infrastructure Engineering.

Quantifying the Effects of Interventions Based on Visual Inspections from a Network of Bridges

Zachary Hamida*and James-A. Goulet
Department of Civil, Geologic and Mining Engineering
Polytechnique Montreal, CANADA

May 8, 2021

Abstract

Network-scale maintenance planning mainly depends on the expected improvement in a structure's condition following an intervention. Quantifying the effect of interventions is commonly based on either the expert judgement and reference values, or ad hoc estimation from visual inspection data. However, visual inspections are subjective and have large variability over time due to the inspectors' uncertainty. State-space models (SSM) have been effectively utilized for quantifying the inspectors uncertainty and modelling the deterioration based on visual inspections. In this study, a new method is proposed to quantify the effect of interventions on structures using the SSM framework. This method allows estimating the local effect of interventions at the structural-element level as well as at the network-scale for a population of structural elements. Moreover, the estimation procedure takes into account the inspectors uncertainty and offers a coherent integration for intervention actions within the deterioration model, in addition to enabling the estimation for the service-life of interventions. The proposed approach is verified using synthetic data and validated using real data taken from inspections and interventions performed on a bridge network in Canada.

Keywords: Effect of Interventions, Visual Inspections, Inspector Uncertainty, Bridge Network Maintenance, State-Space Models, Structural Health Monitoring.

1 Introduction

Interventions are systematic operations that are performed to sustain the serviceability and safety of structures [9]. In the context of network-scale bridge maintenance, an intervention can be classified into three categories, namely are *preventive maintenance*, *rehabilitation* and *replacement* [10, 27]. While one can expect a greater improvement from a rehabilitation

*Corresponding author: zachary.hamida@polymtl.ca

compared to a preventive maintenance, it is important to quantify the effect of each strategy on the condition of structural elements. This is because the network-scale planning of interventions is subject to budgetary constraints that require effective resource allocation [6, 28]. In addition, quantifying the effect of interventions is essential for maintaining the accuracy of deterioration analyses, as it is likely to have multiple interventions during the lifetime of structural elements. In order to quantify the effect of interventions, it is required to have information about the health state of structures before and after applying interventions. Visual inspections are commonly utilized in assessing the health of bridges on a network-scale [17, 22, 4, 18, 11, 26]. Relying on visual inspection data to directly estimate the effect of interventions is insufficient because they are subjective and are based on the judgement of different inspectors [1, 19, 5, 15]. This fact explains the noticeable variability over time in the reported health state of the structural elements [1, 12]. Quantifying the effect of interventions based on visual inspections is traditionally done using a *Discrete Markov Model* (DMM) [8, 6, 7, 24, 23]. The effect of interventions is addressed by two metrics, namely the improvement in the condition and the time delay in the deterioration [8, 23]. These quantities are determined by either relying on the expert judgment [8, 20], or through direct estimation from the inspection data [6, 7, 23]. In either cases, the effect of intervention is characterized by a deterministic value or by three values of minimum, maximum and mode [16, 20]. These representations are insufficient, as applying the same intervention on different structural elements may yield different outcomes [3]. In addition, quantifying the effect of interventions directly from the observations implies disregarding the inspectors uncertainty which is also the case in DMM deterioration models [12]. Accommodating the inspectors uncertainty has been effectively done using state-space models (SSM) [12]. Specifically, the SSM-KR model which is a hybrid framework that combines state-space models (SSM) and kernel regression (KR) [13]. The benefit of using SSM-KR is that it takes advantage of the structural similarity among bridges to improve the deterioration model performance, which makes SSK-KR well suited for short time-series analyses. In this study the effect of interventions is modelled as random variables within the network-scale deterioration model SSM-KR. The proposed formulation enables estimating the local effect of interventions at the structural element level and on the network-scale for a population of structural elements. In addition, it allows accommodating the inspectors uncertainty in the aforementioned estimates. This provides a better understanding for the effect of different types of interventions on a network-scale, which lays the groundwork for improving the planning and allocation of maintenance funds. A byproduct of the proposed framework is to enable the continuity of the deterioration analyses over the lifetime of a structural element, where interventions are coherently integrated within the deterioration framework. Verification and validation of the proposed approach are performed using synthetic and real data respectively. The real data in this study is taken from a network of bridges in Canada.

1.1 Notations

The bridge network is defined by the set $\mathcal{B} = \{b_1, b_2, \ldots, b_{\mathtt{B}}\}$ and the structural attributes of these bridges are defined by $\mathcal{Z} = \{\boldsymbol{z}_1, \boldsymbol{z}_2, \ldots, \boldsymbol{z}_{\mathtt{B}}\}$, whereby $\boldsymbol{z}_j$ is a vector representing the structural attributes of the j-th bridge b_j. The structural elements are defined by the set $\mathcal{E} = \{e_1^j, e_2^j, \ldots, e_{\mathtt{E_j}}^j\}$, where a structural element e_p^j represents the p-th structural element associated with bridge b_j. The set of interventions is defined by $\mathcal{R}^* = \{\mathcal{R}_1, \ldots, \mathcal{R}_j, \ldots, \mathcal{R}_{\mathtt{B_r}}\}$, whereby $\mathcal{R}_j$ represents the interventions performed on bridge b_j. Each intervention is defined by $\mathcal{R}_j = \{\boldsymbol{h}^j, \tau_j\}$, with $\boldsymbol{h}^j = [h_1^j \ \cdots \ h_r^j \ \cdots \ h_{\mathtt{R}}^j]^\intercal$ is a vector of $\mathtt{R}$ intervention categories and τ_j is the intervention time. An intervention category h_r can be applied to one or multiple structural elements in different bridges. In the context of this study, each structural element in the dataset has underwent a single intervention in the time-window of the available data. The deterioration information collected through inspections include the inspection time t, the inspector I_i from the set of inspectors $\mathcal{I} = \{I_1, I_2, \ldots, I_{\mathtt{I}}\}$ responsible for evaluating bridges in $\mathcal{B}$, and the health condition of the structural element $\tilde{y} \in [l, u]$, with l representing the worst possible condition and u representing the best condition. The symbol $(\sim)$ in $\tilde{y}$ is utilized to differentiate between observations in the bounded space $[l, u]$ and unbounded space $\mathbb{R}$ [12].

2 Interventions and Structural Deterioration

In this section, the relation between interventions and deterioration analyses is demonstrated. The formulation of the deterioration model is presented followed by the proposed method for quantifying the effect of interventions.

2.1 Modeling Structural Deterioration

Analyzing the effect of interventions coincides with the deterioration analyses of structural elements. This is because the intervention type h_r is determined by a large extent based on the deterioration state of the structural element. Modelling the deterioration of structural elements in this study is done based on the SSM-KR model [13]. The SSM-KR combines a state-space model (SSM) with kernel regression (KR) to enable analyzing the deterioration behaviour using visual inspection data and structural attributes. The SSM characterizes the deterioration behaviour based on a kinematic model [2], that is defined by the *transition model*,

$$\overbrace{\boldsymbol{x}_t = \boldsymbol{A}\boldsymbol{x}_{t-1} + \boldsymbol{w}_t}^{\text{transition model}}, \ \underbrace{\boldsymbol{w}_t : \boldsymbol{W} \sim \mathcal{N}(\boldsymbol{w}; \boldsymbol{0}, \boldsymbol{Q}_t)}_{\text{process errors}}, \tag{1}$$

where $\boldsymbol{x}_t : \boldsymbol{X} \sim \mathcal{N}(\boldsymbol{x}, \boldsymbol{\mu}_t, \boldsymbol{\Sigma}_t)$ is the state vector at time t, $\boldsymbol{A}$ is the state transition matrix, $\boldsymbol{w}_t$ is the process error with $\boldsymbol{Q}_t$ representing the process error covariance matrix. The state

vector describes the condition x_t, the speed $\dot{x}_t$, and acceleration $\ddot{x}_t$. The inspection data are utilized in updating the state using the *observation model* described by,

$$\overbrace{y_t = \boldsymbol{C}\boldsymbol{x}_t + v_t}^{\text{observation model}}, \underbrace{v_t : V \sim \mathcal{N}(v; 0, \sigma_V^2(I_i))}_{\text{observation errors}}, \tag{2}$$

where y_t represents the observation, $\boldsymbol{C}$ is the observation matrix and $v_t : V \sim \mathcal{N}(v; 0, \sigma_V^2(I_i))$ is the observation error associated with each inspector $I_i \in \mathcal{I}$ performing the inspections. Estimating the hidden states is done using the *Kalman filter* (KF) [14], described by the short form,

$$(\boldsymbol{\mu}_{t|t}, \boldsymbol{\Sigma}_{t|t}, \boldsymbol{\mathcal{L}}_t) = \text{Kalman filter}(\boldsymbol{\mu}_{t-1|t-1}, \boldsymbol{\Sigma}_{t-1|t-1}, \boldsymbol{y}_t, \boldsymbol{A}_t, \boldsymbol{Q}_t, \boldsymbol{C}_t, \boldsymbol{R}_t), \tag{3}$$

where $\boldsymbol{\mu}_{t|t} \equiv \mathbb{E}[\boldsymbol{X}_t|y_{1:t}]$, $\boldsymbol{\Sigma}_{t|t} \equiv \text{cov}[\boldsymbol{X}_t|y_{1:t}]$ represent the posterior expected value and covariance respectively, given observations $\boldsymbol{y}_{1:t}$, and $\boldsymbol{\mathcal{L}}_t$ represents the observations' log-likelihood. The KF state estimates are further refined using the *Kalman smoother* (KS) [21], which improves the estimates based on information from all the observations in a time series. The monotonicity of the deterioration is ensured by constraining the speed estimates to be negative, which is done using the PDF truncation method [25]. Furthermore, a space transformation is performed on the inspection data, using a *transformation function*, to allow the model's predictions and forecasts to be restricted within the range of feasible values, in addition to the uncertainty being dependent on the state [12].
The kernel regression in SSM-KR comes into place for determining the initial deterioration speed. This is done based on a multivariate kernel function $\boldsymbol{k} : \mathbb{R}^{\mathtt{Q}} \to \mathbb{R}$ representing the multiplicative kernel,

$$\boldsymbol{k}\left(\boldsymbol{z}_j, \boldsymbol{Z}_{c(m)}, \boldsymbol{\ell}\right) = k\left(\frac{z_j^1 - \boldsymbol{z}_{c(m)}^1}{\ell_1}\right) \cdot \ldots \cdot k\left(\frac{z_j^{\mathtt{Q}} - \boldsymbol{z}_{c(m)}^{\mathtt{Q}}}{\ell_{\mathtt{Q}}}\right), \; m = 1, \ldots, \mathtt{M}. \tag{4}$$

where $\boldsymbol{Z}_{c(m)} = \left[\boldsymbol{z}_c^1 \; \ldots \; \boldsymbol{z}_c^{\mathtt{Q}}\right] \in \mathbb{R}^{\mathtt{M}^{\mathtt{Q}} \times \mathtt{Q}}$ is a $\mathtt{Q}$-dimensional grid of reference points with $\mathtt{M}$ representing the number of reference points in each dimention, $k(.)$ is a univariate kernel function and $\boldsymbol{\ell} = [\ell_1 \ldots \ell_{\mathtt{Q}}]$ are model parameters associated with each structural attribute. The procedure for estimating the parameters and hidden states related to SSM-KR is detailed in Hamida and Goulet [13].

2.2 Framework for Quantifying the Effect of Interventions

In order to accommodate the effect of interventions in the SSM-KR model, the state vector is augmented to include the following components,

$$\boldsymbol{x}_{p,t}^j = \left[x_{p,t}^j \; \dot{x}_{p,t}^j \; \ddot{x}_{p,t}^j \; \delta_t \; \dot{\delta}_t \; \ddot{\delta}_t\right]^\intercal, \tag{5}$$

where $\boldsymbol{x}_{p,t}^{j}$ is the state vector at time t: $\boldsymbol{X}_t \sim \mathcal{N}(\boldsymbol{\mu}_t, \boldsymbol{\Sigma}_t)$, composed of the vector $[x_{p,t}^{j}\ \dot{x}_{p,t}^{j}\ \ddot{x}_{p,t}^{j}]$ which describes the condition, speed and acceleration components respectively, and the vector $[\delta_t\ \dot{\delta}_t\ \ddot{\delta}_t]$ which represents the changes in the condition, speed and acceleration following an intervention h_r. The effect of an intervention on a structural element is quantified within SSM-KR by modifying the transition model defined in Equation (1) such that,

$$\boldsymbol{x}_t = \boldsymbol{A}_t \boldsymbol{x}_{t-1} + \boldsymbol{w}_t,\ \boldsymbol{w}_t : \begin{cases} \boldsymbol{W}^{\mathtt{ki}} \sim \mathcal{N}(\boldsymbol{0}, \boldsymbol{Q}_t^{\mathtt{ki}}) \\ \boldsymbol{W}^{r} \sim \mathcal{N}(\boldsymbol{0}, \boldsymbol{Q}_t^{r}) \end{cases} \tag{6}$$

The transition matrix $\boldsymbol{A}_t$ is defined by,

$$\boldsymbol{A}_{t=\tau} = \begin{bmatrix} \boldsymbol{A}^{\mathtt{ki}} & \boldsymbol{I}_{3\times3} \\ \boldsymbol{0}_{3\times3} & \boldsymbol{I}_{3\times3} \end{bmatrix},\ \boldsymbol{A}_{t\neq\tau} = \begin{bmatrix} \boldsymbol{A}^{\mathtt{ki}} & \boldsymbol{0}_{3\times3} \\ \boldsymbol{0}_{3\times3} & \boldsymbol{I}_{3\times3} \end{bmatrix}, \tag{7}$$

with $\boldsymbol{I}$ representing the identity matrix and $\boldsymbol{A}^{\mathtt{ki}}$ defined by,

$$\boldsymbol{A}^{\mathtt{ki}} = \begin{bmatrix} 1 & \Delta t & \frac{\Delta t^2}{2} \\ 0 & 1 & \Delta t \\ 0 & 0 & 1 \end{bmatrix}. \tag{8}$$

The full covariance for the transition model errors is described by the matrix $\boldsymbol{Q}_t$ defined as,

$$\boldsymbol{Q}_{t=\tau} = \begin{bmatrix} \boldsymbol{Q}^{\mathtt{ki}} + \boldsymbol{Q}^{r} & \boldsymbol{0}_{3\times3} \\ \boldsymbol{0}_{3\times3} & \boldsymbol{Q}^{r} \end{bmatrix},\ \boldsymbol{Q}_{t\neq\tau} = \begin{bmatrix} \boldsymbol{Q}^{\mathtt{ki}} & \boldsymbol{0}_{3\times3} \\ \boldsymbol{0}_{3\times3} & \boldsymbol{0}_{3\times3} \end{bmatrix}, \tag{9}$$

with $\boldsymbol{Q}^{r}$ and $\boldsymbol{Q}^{\mathtt{ki}}$ defined as,

$$\boldsymbol{Q}^{r} = \mathrm{diag}\left(\left[\sigma_{w_r}^2\ \dot{\sigma}_{w_r}^2\ \ddot{\sigma}_{w_r}^2\right]\right),\ \boldsymbol{Q}^{\mathtt{ki}} = \sigma_w^2 \begin{bmatrix} \frac{\Delta t^5}{20} & \frac{\Delta t^4}{8} & \frac{\Delta t^3}{6} \\ \frac{\Delta t^4}{8} & \frac{\Delta t^3}{3} & \frac{\Delta t^2}{2} \\ \frac{\Delta t^3}{6} & \frac{\Delta t^2}{2} & \Delta t \end{bmatrix}. \tag{10}$$

The standard deviation σ_w characterizes the kinematic model process noise, while $\boldsymbol{\sigma}_{w_r}$ is a vector containing the standard deviations describing the element-level intervention errors. Because of the large variability and limited data in each time-series, it is assumed that the deterioration state of a structural element after an intervention is either staying the same as it was prior to the intervention or is improving by a positive quantity. Consequently, the expected deterioration speed at time $t = \tau$ is bounded with $\dot{\mu}_\tau \in [\dot{\mu}_{\tau-1}, 0]$ and similarly for the acceleration $\ddot{\mu}_\tau \in [\ddot{\mu}_{\tau-1}, 0]$. In order to accommodate the aforementioned bounds, the following state constraints are applied in the KF,

$$\begin{aligned} \dot{\mu}_{\tau-1} \leq & \dot{\mu}_\tau \leq 0, \\ \ddot{\mu}_{\tau-1} - \ddot{\sigma}_{\tau-1} \leq & \ddot{\mu}_\tau \leq \ddot{\sigma}_{\tau-1}. \end{aligned} \tag{11}$$

The acceleration is allowed to be positive to accommodate cases where the acceleration is slightly positive or near zero at the time step before the intervention $t = \tau - 1$. This implies that the deterioration speed was declining at that point in time. In order to ensure the consistency in the model, the state constraints are also applied in the KS after changing the bounds as in,

$$\begin{aligned} \dot{\mu}_\tau \leq & \dot{\mu}_{\tau+1}, \\ \ddot{\mu}_\tau \leq & \ddot{\mu}_{\tau+1} + \ddot{\sigma}_{\tau+1}. \end{aligned} \tag{12}$$

The state constraints are only examined at the transition from time $t = \tau - 1$ to time $t = \tau$ or reversely; if one of the constraints is violated, the PDF truncation method is applied [25].

2.3 State Estimation and Model Parameters

The hidden state δ_t, $\dot{\delta}_t$ and $\ddot{\delta}_t$ that represent the network-scale effects of interventions are estimated based on sequential updating from the inspection data. For a given type of intervention $h_r \in \mathcal{R}$, the expected value for each component is initially set to zero $\mu_t^\delta = \mu_t^{\ddot{\delta}} = 0$, except for the speed $\mu_t^{\dot{\delta}}$. This is because assigning $\mu^{\dot{\delta}_t} \approx 0$ can trigger the state constraints defined in Equation (11), resulting in truncating the PDF of the state at an early stage. After the initialization step, the intervention quantification framework presented in §2.2 is applied, through which the states δ_t, $\dot{\delta}_t$ and $\ddot{\delta}_t$ are updated based on the inspection data before and after intervention h_r on element e_p^j. The updated state is then utilized in the analyses of structural element e_{p+1}^j which allows the states δ_t, $\dot{\delta}_t$ and $\ddot{\delta}_t$ to be updated with another set of inspections before and after intervention h_r. The sequential updates are carried out up to the last structural element with the intervention h_r. Therefore, the estimation quality for quantifying the effect of an intervention type depends on the number of structural elements that underwent the same type of intervention. Following the update from the data of the last structural element, the updated states δ_t, $\dot{\delta}_t$ and $\ddot{\delta}_t$ can be utilized in modelling the element-level interventions within the SSM-KR framework. The parameters associated with the intervention quantification framework are defined in the set $\boldsymbol{\theta}_r = \{\sigma_{w_r}, \dot{\sigma}_{w_r}, \ddot{\sigma}_{w_r}, \sigma_{h_r}, \dot{\sigma}_{h_r}, \ddot{\sigma}_{h_r}\}$, where $\sigma_{h_r}, \dot{\sigma}_{h_r}, \ddot{\sigma}_{h_r}$ are the standard deviations associated with the prior knowledge for the states δ_t, $\dot{\delta}_t$ and $\ddot{\delta}_t$ at the beginning of the sequential estimation process. The subscript in $\boldsymbol{\theta}_r$ is a reference to the intervention category h_r, which implies that each intervention category has its own set of parameters. The estimation for the aforementioned parameters is done using the *Maximum Likelihood Estimate* (MLE). The network-scale log-likelihood [12] is,

$$\mathcal{L}(\boldsymbol{\theta}_r) = \sum_{j=1}^{\mathtt{B}_r} \sum_{p=1}^{\mathtt{E}_r^j} \sum_{t=1}^{\mathtt{T}_p} \ln f(y_{t,p}^j | y_{1:t-1,p}^j, \boldsymbol{\theta}_r), \tag{13}$$

where $\mathtt{B}_r$, $\mathtt{E}_r^j$ are the total number of bridges and structural elements respectively, that underwent intervention h_r, and $\mathtt{T}_p$ is the number of observation per time series. The

parameters estimation problem is defined as,

$$\begin{aligned} \boldsymbol{\theta}_r^* = \arg\max_{\boldsymbol{\theta}_r} \quad & \mathcal{L}(\boldsymbol{\theta}_r), \\ \text{subject to:} \quad & \sigma_{w_r}, \dot{\sigma}_{w_r}, \ddot{\sigma}_{w_r} > 0, \\ & \sigma_{h_r}, \dot{\sigma}_{h_r}, \ddot{\sigma}_{h_r} > 0. \end{aligned} \tag{14}$$

Solving the optimization problem defined above is possible using gradient-based optimization methods such as *Newton-Raphson* [12].

3 Interventions & Inspections Database

In this section, a dataset of real interventions and inspections is introduced, in addition to discussing the details of synthetic inspections and interventions dataset generated to verify the model performance.

3.1 Database for the Real Case Study

The real database is composed of visual inspections, structural attributes and intervention data for a network of $\mathtt{B} \approx 10000$ bridges located in the province of Quebec, Canada. The network-scale interventions are categorized as h_1: preventive maintenance, h_2: routine maintenance and h_3: repairs [18]. The aforementioned interventions are performed based on either a health condition threshold being violated or a recommendation from the inspector. Moreover, the visual inspections of structural elements are reported based on 4 categories of damage severity, A: *Nothing to little*, B: *Medium*, C: *Important* and D: *Very Important* [18]. The inspectors report the percentage of a structural element's area that belongs to each of damage categories, such that $0\% \leq y_a, y_b, y_c, y_d \leq 100\%$, and $y_a + y_b + y_c + y_d = 100\%$. An example of visual inspection is : $y_a = 60\%,\ y_b = 20\%,\ y_c = 10\%,\ y_d = 10\%$, implying that 60% of the structural element area has no damage, 20% has medium damage, 10% has important damage and 10% has very important damage. Representing the 4 categories into a single metric is done by combining them using a weighted sum,

$$\tilde{y} = \omega_1 y_a + \omega_2 y_b + \omega_3 y_c + \omega_4 y_d, \tag{15}$$

with $\omega_1 = 100$, $\omega_2 = 75$, $\omega_3 = 50$, $\omega_4 = 25$ representing the utilities and $\tilde{y}$ is the aggregated observation [12]. This aggregation allows the deterioration condition of structural elements to be a continuous numerical value with $\tilde{y} \in [25, 100]$, where $\tilde{y} = 100$ is equivalent to a perfect health state and $\tilde{y} = 25$ is equivalent the worst health state (e.g. $y_a = 0\%, y_b = 0\%, y_c = 0\%, y_d = 100\%$).

3.2 Simulating Interventions and Synthetic Data

Synthetic data is generated in order to verify the proposed framework performance, provided that the true effect of interventions is known. Therefore, the synthetic dataset is ensured to be similar to the real data, both quantitatively and qualitatively. Simulating the interventions is done according to two factors; the structure priority, and the deterioration state. The priority factor is assigned to structures randomly, based on a uniform distribution $\Omega \sim \mathcal{U}(1,3)$. The aforementioned factor emulates the inspector's recommendation for performing an intervention in the real case. The type of intervention is determined using a synthetic decision making system defined by if-then rules, which are detailed in Appendix 1. In total, four synthetic intervention actions are defined, h_0: do nothing, h_1: preventive maintenance, h_2: repairs and h_3: major repairs. Whenever one of the actions $h_{1:3}$ is applied, the timing of the synthetic intervention is recorded. The true improvement associated with each type of intervention is modeled by a Normal distribution with parameters defined in Table 1.

Table 1: Types of synthetic interventions with their corresponding expected improvement represented by an expected value and a standard deviation.

Type	μ_δ	σ_δ	$\mu_{\dot{\delta}}$	$\sigma_{\dot{\delta}}$	$\mu_{\ddot{\delta}}$	$\sigma_{\ddot{\delta}}$
h_1	0	10^{-4}	0.2	0.05	0	10^{-4}
h_2	7.5	2	0.3	0.1	0	10^{-4}
h_3	18.75	4	0.4	0.15	0	10^{-4}

For simulating the deterioration state, the true state is generated using the transition model with $\sigma_w = 5 \times 10^{-3}$ as defined in Equation (1). Thereafter, the observations are generated based on the observation model described in Equation (2), with each inspector $I_i \in \mathcal{I}$ having a standard deviation generated from a Uniform distribution $\sigma_V(I_i) \sim \mathcal{U}(1,6)$. The deterioration state in the synthetic data is represented by a continuous numerical value with $\tilde{y} \in [25, 100]$, with each structural element having an average service life of 60 years. The majority of structural elements have 3 to 5 observations over time, while few structural elements have 8-10 observations. Moreover, we ensured that there is at least one observation before or after the intervention. As for the synthetic structural attributes, a single attribute is considered and defined by the following relation,

$$z_j = 10 \times |\dot{x}_0^j| + 4 + w_0 : W_0 \sim \mathcal{N}(w_0; 0, 0.5^2). \tag{16}$$

The other characteristics and thresholds that are required in order to simulate realistic data are inherited from the measures defined by [12].

4 Case Studies

In this section, the performance of the proposed framework is verified using synthetic data and thereafter validated with real data.

4.1 Model Verification Using Synthetic Data

The synthetic dataset is composed of $\mathtt{E} = 17000$ structural elements with a total of $\mathtt{E}_r = 414$ structural elements that underwent interventions belonging to categories $h_{1:3}$. The observations in the synthetic dataset are obtained from $\mathtt{I} = 223$ inspectors. The structural elements without interventions are utilized for training the SSM-KR deterioration model. Thereafter, the pre-trained deterioration model is utilized for modelling interventions as described in §2.2. The optimized model parameters $\boldsymbol{\theta}_{1:3}$ for each intervention category are shown in Table 2. The state estimation for δ and $\dot{\delta}$ using the proposed framework with

Table 2: Estimated model parameters for synthetic interventions.

Intervention	σ_{w_r}	$\dot{\sigma}_{w_r}$	$\ddot{\sigma}_{w_r}$	σ_{h_r}	$\dot{\sigma}_{h_r}$	$\ddot{\sigma}_{h_r}$
h_1	1.42	0.03	0.01	0.26	0.79	0.09
h_2	3.10	0.79	0.05	6.77	0.63	0.03
h_3	3.82	0.75	0.04	9.82	0.78	0.002

parameters $\boldsymbol{\theta}_{1:3}$ are shown in Figure 1. In this graph, the expected change in the condition μ^{δ} converges to the true change δ in each of the intervention categories $h_{1:3}$. Moreover, the state estimations shows that the proposed framework provides reliable estimates with as little as 20 structural elements with interventions. On the other hand, the estimate for the change in the deterioration speed $\dot{\delta}$ is not as accurate as the condition estimates δ. The limited performance in estimating $\dot{\delta}$ is noticeable in the case of intervention category h_3. The main reasons for the limited predictive capacity of $\dot{\delta}$ are: the fact that the deterioration speed is not directly observed and there are few observations before and/or after the intervention. As for interventions of type h_3, this category of interventions is mainly applied on structures having an average health condition, which is associated with a higher uncertainty in the estimates of the deterioration state [12]. Nonetheless, if the number of observations before and/or after the intervention is sufficient, the state estimation of $\dot{\delta}$ converges to the true value. An example that demonstrates the effect of the number of observations on $\mu^{\dot{\delta}}$ is shown in Figure 2. In this example, the expected value $\mu^{\dot{\delta}}$ for the intervention h_3 approaches the true change as the number of observations per time series increases. Although estimating $\dot{\delta}$ is limited for interventions of type h_3, the resulting state $\dot{\delta}$ can be considered as a good initial estimate for the intervention at the structural element level. This initial estimate is subsequently updated according to the data of each structural element using the KS. This is demonstrated in Figures 3-5, with examples of time

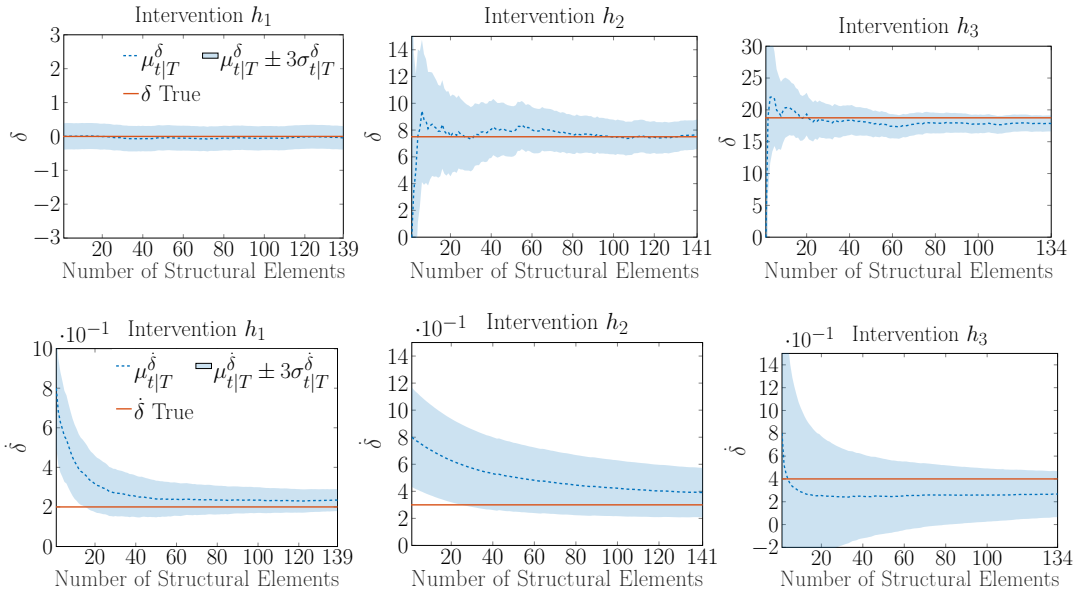

Figure 1: Recursive estimation for the network-scale change in the deterioration condition δ and speed $\dot{\delta}$ based on data from $\mathtt{E}_1 = 139$ structural elements underwent intervention h_1, $\mathtt{E}_2 = 141$ elements underwent intervention h_2, and $\mathtt{E}_3 = 134$ elements underwent intervention h_3.

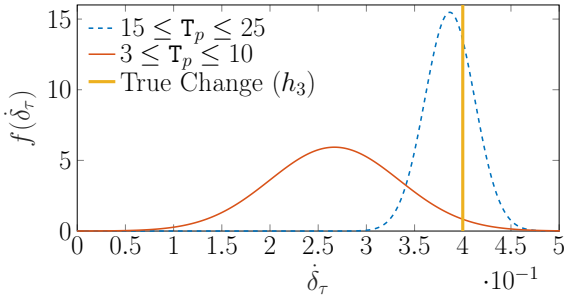

Figure 2: The effect of the number of observations per time series $\mathtt{T}_p$ on the state estimate of $\dot{\delta}_\tau$ under the same intervention h_3 at time $\tau \approx \frac{\mathtt{T}_p}{2}$.

series for synthetic structural elements. Figure 3 illustrates an example of a deterioration behaviour with an intervention h_1. In this example, the true deterioration state before and after the intervention is within the confidence interval of the model, despite having a single observation before the intervention. Another example shown in Figure 4, illustrates the model performance in the case of synthetic structural element with an intervention of category h_2. In this case, the estimate of the deterioration state is consistent with the

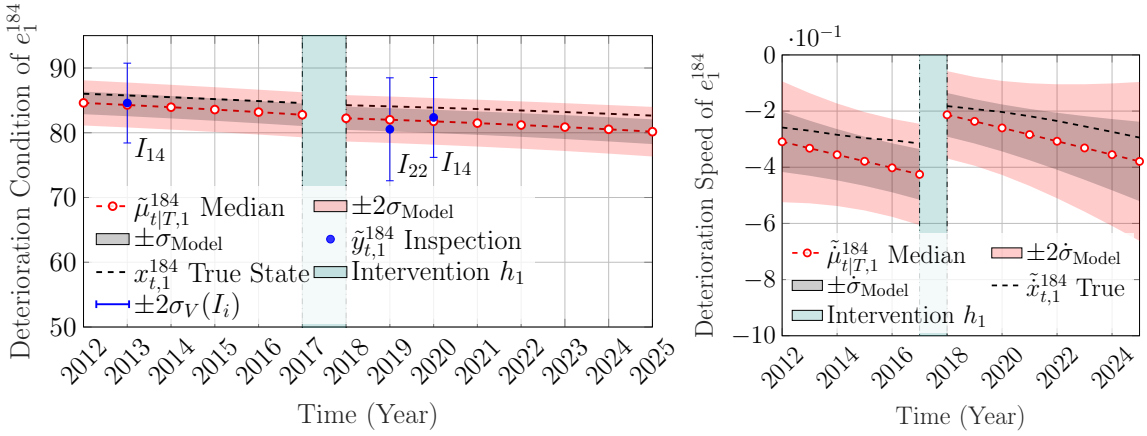

Figure 3: Deterioration state analysis for the condition and the speed based on the observations $\tilde{\boldsymbol{y}}_{t,1}^{184} \in [25, 100]$ of the synthetic structural element e_1^{184} with an intervention h_1 at time $\tau = 2018$ and error bars representing the inspectors' uncertainty estimates.

true state of the speed and the condition even though a single observation exist after the intervention.

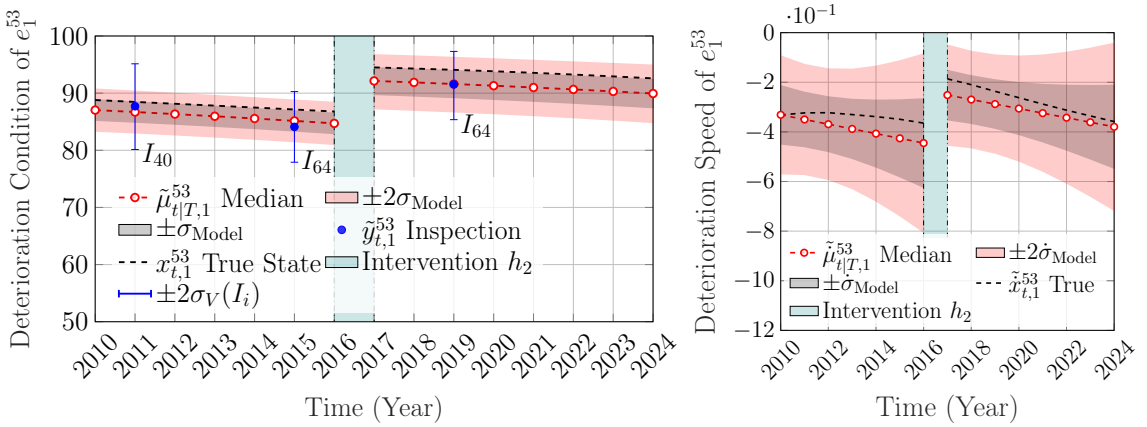

Figure 4: Deterioration state analysis for the condition and the speed based on the observations $\tilde{\boldsymbol{y}}_{t,1}^{53} \in [25, 100]$ of the synthetic structural element e_1^{53} with an intervention h_2 at time $\tau = 2017$ and error bars representing the inspectors' uncertainty estimates.

The last time series example from the synthetic dataset is shown in Figure 5, where the model performance is examined in a structural element with intervention of category h_3. This example shows that although the capacity of estimating $\dot{\delta}$ is limited for this intervention category, the proposed framework has yielded an acceptable performance in estimating

the deterioration state, verified by the true state being within the confidence interval of the model estimates. In order to examine the modelling capacity of interventions for the

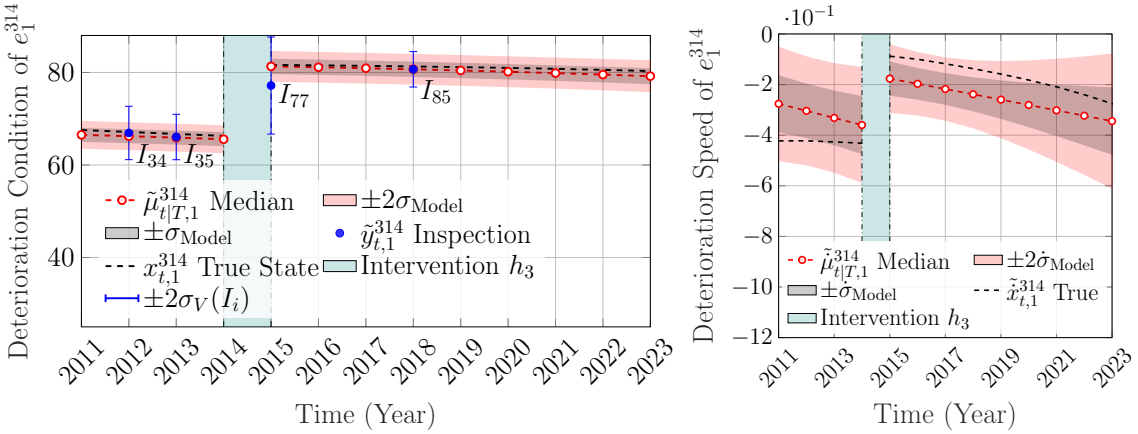

Figure 5: Deterioration state analysis for the condition and the speed based on the observations $\tilde{\boldsymbol{y}}^{314}_{t,1} \in [25, 100]$ of the synthetic structural element e_1^{314} with an intervention h_3 at time $\tau = 2015$ and error bars representing the inspectors' uncertainty estimates.

entire population of synthetic structural elements, the errors in the state estimates after an intervention are examined. Table 3 shows the expected errors in the deterioration condition $\mathbb{E}[\epsilon] = \mu_{\tau|T} - x_\tau$, and the deterioration speed $\mathbb{E}[\dot{\epsilon}] = \dot{\mu}_{\tau|T} - \dot{x}_\tau$, alongside the standard deviations σ_ϵ, $\dot{\sigma}_\epsilon$ and the skewness γ and $\dot{\gamma}$ for the condition and the speed respectively. The error estimates reported in Table 3 show that for a sample of $\mathtt{E_r} = 414$

Table 3: The error in the state estimate following an intervention represented by the expected error ± standard deviation and skewness γ for a sample of 414 synthetic structural elements.

Intervention	$\mathbb{E}[\epsilon] \pm \sigma_\epsilon$	γ	$\mathbb{E}[\dot{\epsilon}] \pm \dot{\sigma}_\epsilon$	$\dot{\gamma}$
h_1	-0.22 ± 1.62	-0.09	0.04 ± 0.12	0.38
h_2	$+0.09 \pm 1.75$	-0.34	0.09 ± 0.13	0.01
h_3	-0.54 ± 2.29	0.05	0.10 ± 0.15	0.38

synthetic structural elements, the distribution of errors is approximately symmetric (i.e. $-0.5 < \gamma < 0.5$), and that the bias in the estimates is insignificant compared to the range of values of which the speed and the condition can take. Moreover, it is noticed that the estimated error increases with major interventions (i.e. h_3 vs. h_1), this is attributed to the fact that major interventions are applied to structures in an average health condition, which is associated with increase in the uncertainty of the deterioration state estimates

[12]. An additional advantage for the proposed method is that it allows estimating the service-life of an intervention t_h, which represents the number of years before returning to the original state prior to intervention h_r. This can be done by estimating the probability of crossing the original state, from the cumulative distribution function (CDF) at each year after the intervention using,

$$F(t_h|h_r) = \Pr(X_{\tau+t} \leq x_{\tau-1}|h_r),\ \forall t \in \mathbb{Z}_0^+. \tag{17}$$

The probability density function $f(t_h|h_r)$ can be obtained by differentiating the CDF in Equation 17. In order to demonstrate the estimation of the service-life t_h, consider the time series example shown in Figure 4. Estimating the service-life of intervention h_2 can be done by computing $F(t_h|h_2)$ and $f(t_h|h_2)$, which yields the probability distribution shown in Figure 6.

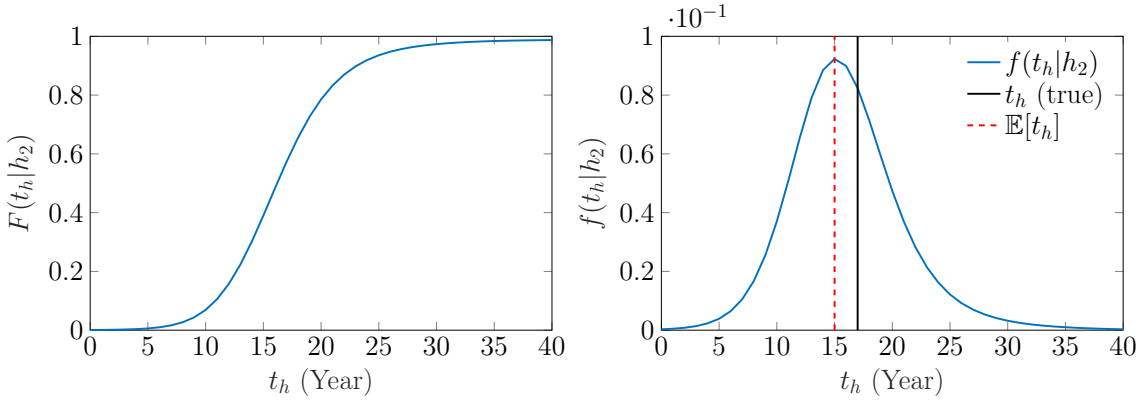

Figure 6: The cumulative distribution and probability density functions for the time before returning to the original condition state prior to intervention h_2 on synthetic structural element e_1^{53}, with $\mathbb{E}[t_h]$ representing the expected time of the return, and t_h(true) representing the true time of the return.

Based on the PDF shown in Figure 6, the number of years before returning to the original state is $\mathbb{E}[t_h] = 15$ years, which is near the true return $t_h(\text{true}) = 17$ years. The single case estimate can be generalized to include all elements that underwent the same type of intervention h_2, by computing the expected probability $\mathbb{E}[f(t_h|h_2)]$ at each year. Consequently, the PDF associated with intervention h_2 for a population of synthetic structural elements can be obtained as shown in Figure 7. This PDF is verified with the normalized histogram for the true service-life of the synthetic structural elements.
It should be noted that estimating the service-life t_h of intervention h_r, depends mainly on the capacity to perform long-term forecasts. Therefore, factors that affect the long-term forecast (e.g., 2-3 inspections per element), would also affect the estimation of t_h.

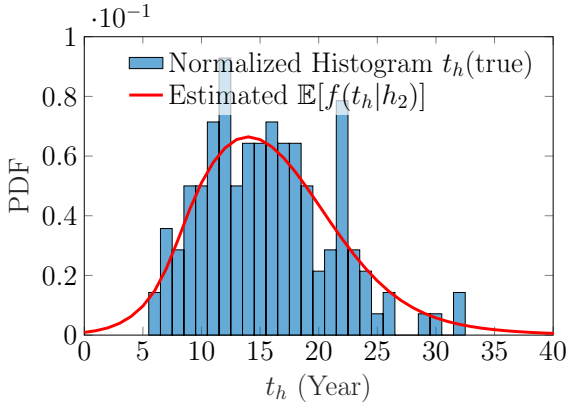

Figure 7: Comparison between the estimated probability density function and the normalized histogram for the true returning time to the original state prior to intervention h_2, based on a population of synthetic structural elements $\mathtt{E}_2 = 141$.

4.2 Model Validation Using Real Data

Analyses with real data involves two types of structural element; the *front walls* and the *beams* of different bridges. The first dataset consists in the interventions and inspections for *front walls* which is classified as an abutment element [18]. This dataset includes a total $\mathtt{E} = 16360$ structural elements taken from $\mathtt{B} = 8278$ bridges. The subset of bridges that underwent interventions is composed of $\mathtt{B}_r = 193$ bridges with $\mathtt{E}_r = 319$ *front wall* structural elements. The type of interventions involved in the analyses on *front walls* are categorized according to the structures' inspection manual [18]. The first intervention category h_2 is composed of activities that relate to strengthening and consolidation. The second intervention category h_3 includes a variety of repair activities, such as the repair of concrete elements and masonry wall elements. Quantifying the effect of the aforementioned intervention categories is done using the proposed framework. The estimated model parameters for each category of interventions are shown in Table 4.

Table 4: Estimated model parameters for interventions on the *front wall* structural elements.

Intervention	σ_{w_r}	$\dot{\sigma}_{w_r}$	$\ddot{\sigma}_{w_r}$	σ_{h_r}	$\dot{\sigma}_{h_r}$	$\ddot{\sigma}_{h_r}$
h_2	6.03	0.05	0.02	5.00	0.27	0.03
h_3	9.34	0.05	0.01	9.99	0.31	0.02

The recursive state estimation for the expected improvement in the condition δ and speed $\dot{\delta}$ are shown in Figure 8.
In Figure 8, the network-scale improvement in the condition from applying h_2 interventions is $\mu_2^\delta = 13.57$ with $\sigma_2^\delta = 1.38$ compared to $\mu_3^\delta = 17.56$ with $\sigma_3^\delta = 1.28$ gained from applying

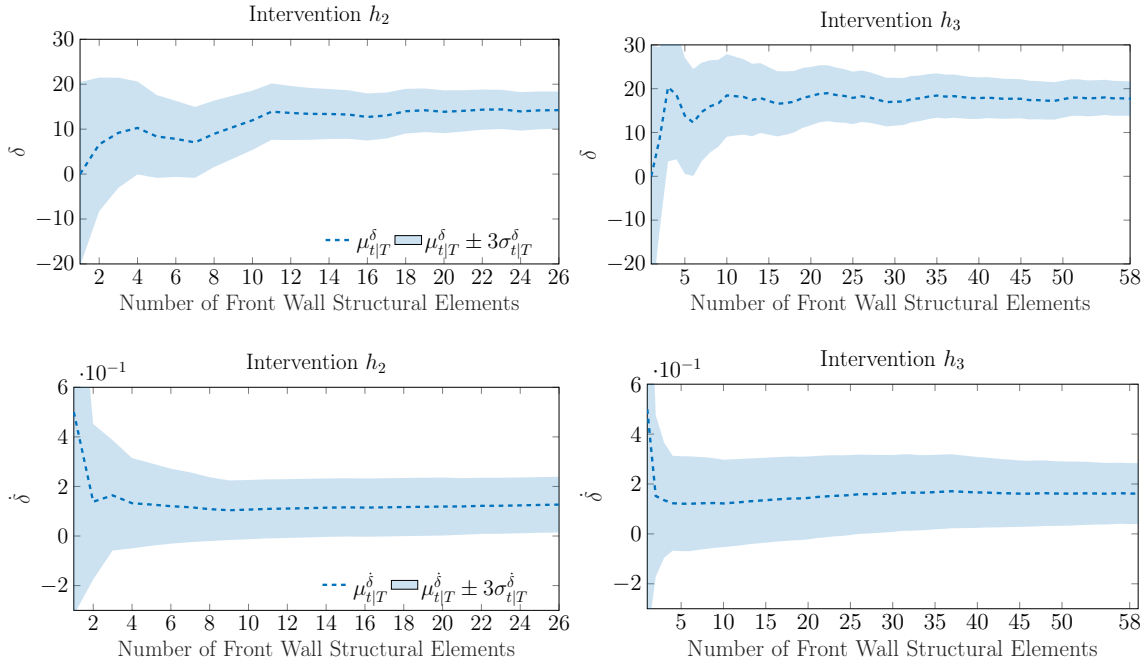

Figure 8: Recursive estimation for the network-scale change in the deterioration condition and speed of the *front wall* structural elements, using data from $\mathtt{E}_2 = 26$ elements that underwent intervention h_2, and $\mathtt{E}_3 = 58$ elements that underwent intervention h_3.

h_3 interventions. Similarly, the deterioration speed improvement for h_3 interventions is $\mu^{\dot{\delta}}_3 = 0.16$ with $\sigma^{\dot{\delta}}_3 = 0.05$, which is better than h_2 interventions with $\mu^{\dot{\delta}}_2 = 0.13$ and $\sigma^{\dot{\delta}}_2 = 0.06$. It should be noted that in cases where there are two (or more) types of interventions that are frequently applied together and at the same time, the recursive estimation framework can provide the prior estimate for the effect of intervention based on data from such instances only. However, with the limited amount of intervention data currently available, the combination between interventions is not considered. Examples of time series analyses for structural elements that underwent an intervention from each category are shown in Figures 9-10. Figure 9 shows an example of a *front wall* structural element that underwent intervention of type h_2.

From Figure 9, the estimate of the deterioration condition before the intervention has a lower uncertainty due to the observation from an inspector with a low uncertainty. The second time series example, shown in Figure 10, is for a concrete *front wall* element that underwent repairs activities from interventions category h_3. In Figure 10 it is noticed that the deterioration speed estimate has a high uncertainty before the intervention compared to the estimate after the intervention. This is justified by the fact that a single observation is

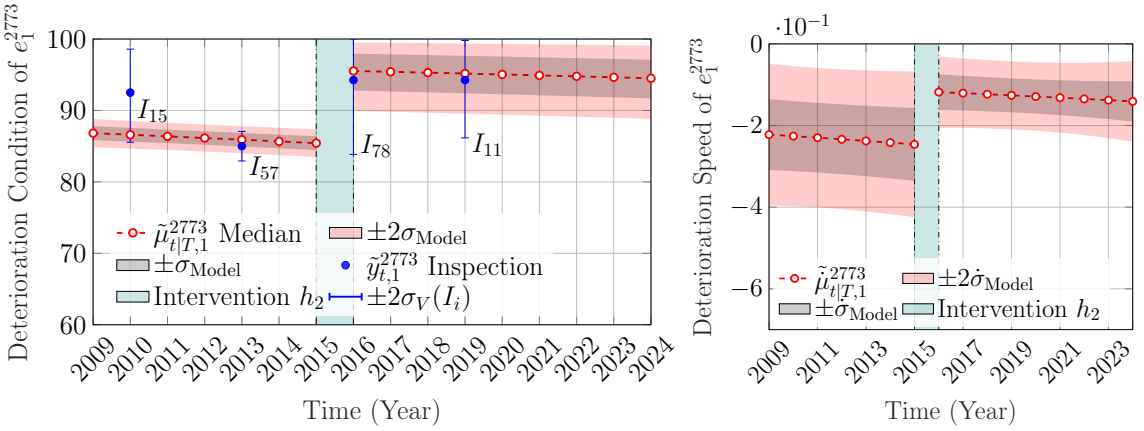

Figure 9: Deterioration state analysis for the condition and the speed based on the observations $\tilde{\boldsymbol{y}}_{t,1}^{2773} \in [25, 100]$ of the *front wall* structural element e_1^{2773} with an intervention h_2 at time $\tau = 2016$ and error bars representing the inspectors' uncertainty estimates.

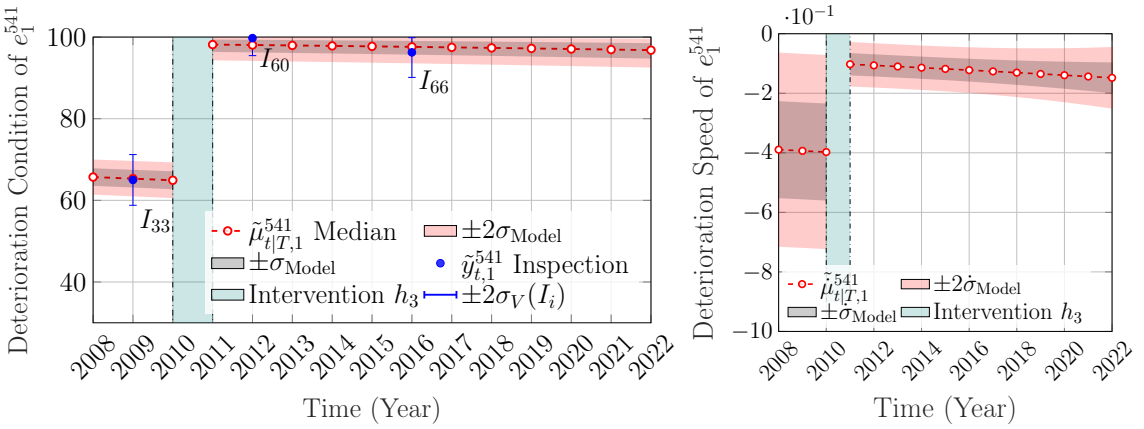

Figure 10: Deterioration state analysis for the condition and the speed based on the observations $\tilde{\boldsymbol{y}}_{t,1}^{541} \in [25, 100]$ of the *front wall* structural element e_1^{541} with an intervention h_3 at time $\tau = 2011$ and error bars representing the inspectors' uncertainty estimates.

available before the intervention compared to two observations after; in addition, if the state estimate of the deterioration speed is near zero (upper bound), this estimate is ensured to be nonpositive using the monotonicity constraint $\dot{\mu}_{t,p}^{j} + 2\dot{\sigma}_{t,p}^{j} \leq 0$ [12], if this constraint is violated, the PDF of the speed is truncated using the PDF truncation method [12, 25]. The service-life t_h of interventions h_2 and h_3, for the *front wall* elements are reported by the CDFs shown in Figure 11. The CDFs are estimated based on the data from $\mathtt{E}_2 = 26$

structural elements for h_2 interventions, and $\mathtt{E}_3 = 58$ structural elements for h_3 interventions. In Figure 11, the CDF associated with h_3 interventions has a flatter curve compared to the

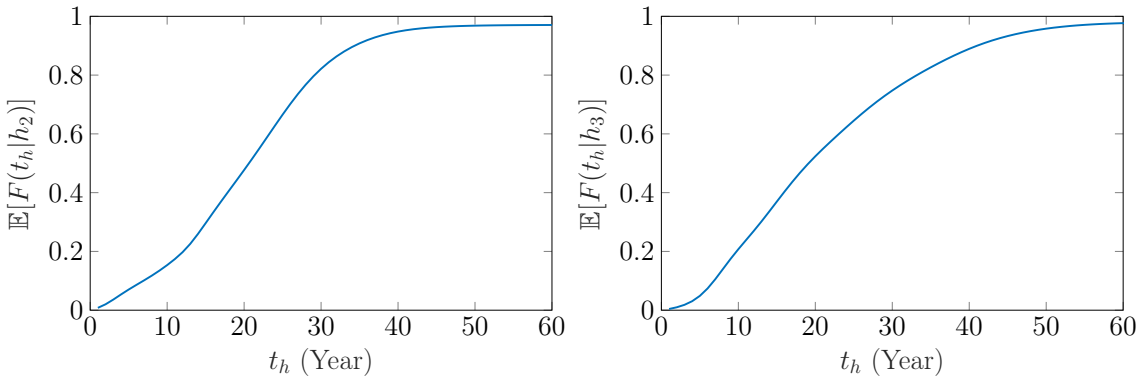

Figure 11: Cumulative distribution functions for the service-life t_h of intervention h_2 (left), and intervention h_3 (right), based on data from *front wall* structural elements.

CDF associated with h_2 interventions. This implies that overall, h_3 interventions have a service-life t_h grater than h_2 interventions, which coincides with the overall improvement results shown in Figure 8.

The second database consists in the inspections and interventions of *beam* structural elements. This dataset includes a total of $\mathtt{E} = 24824$ structural elements from $\mathtt{B} = 2881$ bridges. The number of bridges that underwent interventions on *beams* is $\mathtt{B}_r = 95$, with $\mathtt{E}_r = 485$ *beam* structural elements. A single intervention category h_3 is examined with activities that includes repair works for concrete and steel *beam* elements [18]. The estimated model parameters associated with h_3 are reported in Table 5.

Table 5: Estimated model parameters for interventions on the *beam* structural elements.

Intervention	σ_{w_r}	$\dot{\sigma}_{w_r}$	$\ddot{\sigma}_{w_r}$	σ_{h_r}	$\dot{\sigma}_{h_r}$	$\ddot{\sigma}_{h_r}$
h_3	5.68	0.06	0.01	6.75	0.12	0.02

The hidden state estimation for the expected improvement in the condition and the speed are shown in Figure 12. From this figure, it is noticed that the network-scale expected improvement in the condition is $\mu_3^{\delta} = 12.61$ with $\sigma_3^{\delta} = 0.77$, while the improvement in the speed is $\mu_3^{\dot{\delta}} = 0.28$ with $\sigma_3^{\dot{\delta}} = 0.06$.

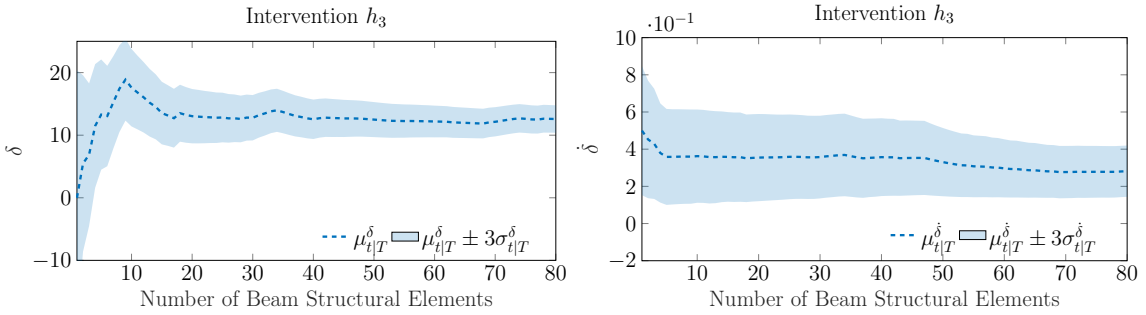

Figure 12: Recursive estimation for the network-scale change in the deterioration condition and speed based on $\mathtt{E}_3 = 80$ *beam* structural elements that underwent intervention h_3.

An example of *beam* structural element that underwent repairs of type h_3 is shown in Figure 13. In this example, the condition and speed state estimates show improvements in the health state of structural element e_1^{520}, following the intervention at year $\tau = 2011$.

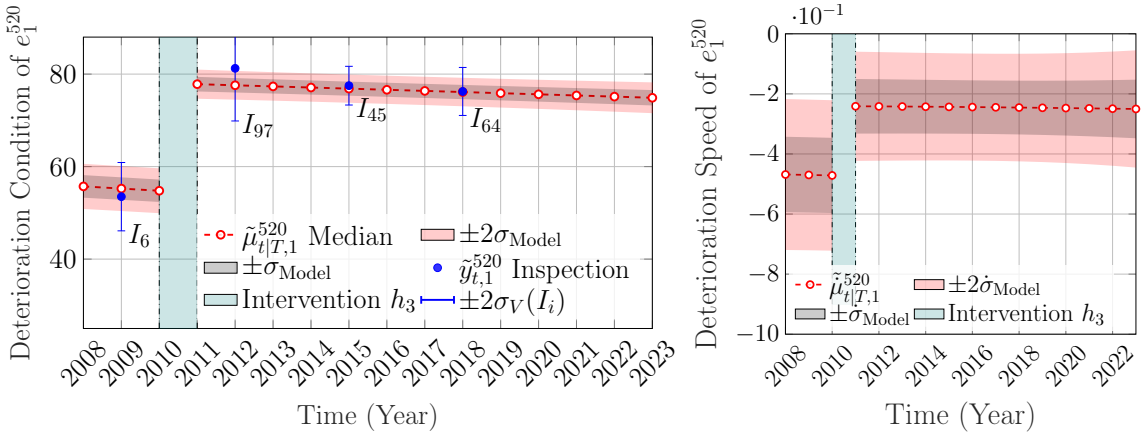

Figure 13: Deterioration state analysis for the condition and the speed based on the observations $\tilde{\boldsymbol{y}}^{520}_{t,1} \in [25, 100]$ of the *beam* structural element e_1^{520} with an intervention h_3 at time $\tau = 2011$ and error bars representing the inspectors' uncertainty estimates.

Moreover, the service-life t_h associated with h_3 interventions on *beam* elements is illustrated by the CDF shown in Figure 14.

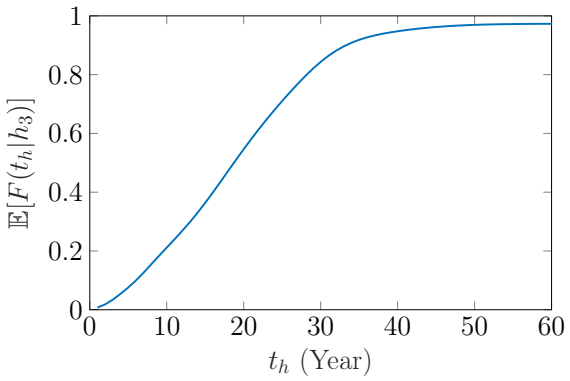

Figure 14: Cumulative distribution function for the service-life t_h of intervention h_3, based on data from $\mathtt{E}_3 = 80$ *beam* structural elements.

5 Conclusions

In this paper, the effect of interventions is quantified as random variable based on visual inspections. The proposed recursive quantification framework is integrated within a deterioration model SSM-KR. The performance of the quantification framework is verified with synthetic data that emulates real data with interventions, followed by validation using cases from real data. The verification results demonstrated the predictive capacity with the true expected improvements being within the confidence interval of the model estimates, for each intervention category. Furthermore, the error in the deterioration state estimate following an intervention is reported for a sample of synthetic structural elements. The error estimates have shown that major repairs have a larger error after an intervention. This is justified by the fact that the deterioration state estimates have a larger uncertainty in structures with an average health condition. This limitation can be surpassed if more observations become available. The proposed framework have also shown the capacity to estimate the service-life of interventions, based on a single structural element and a population of structural elements. Furthermore, the proposed framework is validated with real data that includes two types of structural elements, namely *front walls* and *beams* structural elements. The validation involved estimating the expected improvement following different intervention categories as well as time series analyses for individual structural elements, in addition to estimating the service-life for each type of intervention. The analyses with real data have shown a similar performance in comparison with the synthetic data. In summary, the proposed framework enables estimating the effect of interventions, locally and on network-scale, as random variables. This lays the ground work for performing probabilistic life-time deterioration analyses, risk analyses, and interventions planning.

Acknowledgements

This project is funded by the Transportation Ministry of Quebec Province (MTQ), Canada. The authors would like to acknowledge the support of René Gagnon for facilitating the access to the inspections database employed in this paper.

References

[1] Duzgun Agdas, Jennifer A Rice, Justin R Martinez, and Ivan R Lasa. Comparison of visual inspection and structural-health monitoring as bridge condition assessment methods. *Journal of Performance of Constructed Facilities*, 30(3):04015049, 2015.

[2] Yaakov Bar-Shalom, X Rong Li, and Thiagalingam Kirubarajan. *Estimation with applications to tracking and navigation: theory algorithms and software*. John Wiley Sons, 2004.

[3] Paolo Bocchini and Dan M Frangopol. A probabilistic computational framework for bridge network optimal maintenance scheduling. *Reliability Engineering System Safety*, 96(2):332–349

[4] Miryam Cabieses, Andrew Mikhail, and Namra Khan. Design of a bridge inspection system (bis) to reduce time and cost. Technical report, Department of Systems Engineering and Operations Research George in Mason University, 2014.

[5] Leslie E Campbell, Robert J Connor, Julie M Whitehead, and Glenn A Washer. Benchmark for evaluating performance in visual inspection of fatigue cracking in steel bridges. *Journal of Bridge Engineering*, 25(1):04019128

[6] Dilum Fernando, Bryan T Adey, and Scott Walbridge. A methodology for the prediction of structure level costs based on element condition states. *Structure and Infrastructure Engineering*, 9(8):735–748

[7] Dilum Fernando, Bryan T Adey, and Nam Lethanh. A model for the evaluation of intervention strategies for bridges affected by manifest and latent deterioration processes. *Structure and Infrastructure Engineering*, 11(11):1466–1483

[8] Cláudia Ferreira, Luís Canhoto Neves, José C Matos, and José Maria Sousa Soares. A degradation and maintenance model: Application to portuguese context. *Proceedings of Bridge Maintenance, Safety, Management and Life Extension*, pages 483–489, 2014.

[9] FHWA. *Title 23 United States Code*. Federal Highway Administration, 2012.

[10] FHWA. *Bridge Preservation Guide Maintaining a Resilient Infrastructure to Preserve Mobility*. U.S. Department of transportation Federal Highway Administration, 2018.

[11] Farzad Ghodoosi, Ashutosh Bagchi, and Tarek Zayed. System-level deterioration model for reinforced concrete bridge decks. *Journal of Bridge Engineering*, 20(5):04014081

[12] Zachary Hamida and James-A Goulet. Modeling infrastructure degradation from visual inspections using network-scale state-space models. *Structural Control and Health Monitoring*, 2020.

[13] Zachary Hamida and James-A Goulet. Network-scale deterioration modelling of bridges based on visual inspections and structural attributes. *Structural Safety*, 88:102024 2020.

[14] Rudolf Emil Kalman. Contributions to the theory of optimal control. *Bol. Soc. Mat. Mexicana*, 5(2):102–119, 1960.

[15] Zhe Li and Rigoberto Burgueño. Using soft computing to analyze inspection results for bridge evaluation and management. *Journal of Bridge Engineering*, 15(4):430–438

[16] Min Liu and Dan M Frangopol. Bridge annual maintenance prioritization under uncertainty by multiobjective combinatorial optimization. *Computer-Aided Civil and Infrastructure Engineering*, 20(5):343–353

[17] Mark Moore, Brent M Phares, Benjamin Graybeal, Dennis Rolander, and Glenn Washer. Reliability of visual inspection for highway bridges, volume i. Technical report, Turner-Fairbank Highway Research Center, 6300 Georgetown Pike, 2001.

[18] MTQ. *Manuel d'Inspection des Structures*. Ministère des Transports, de la Mobilité Durable et de l'Électrification des Transports, Jan 2014.

[19] Eugene OBrien, Ciaran Carey, and Jennifer Keenahan. Bridge damage detection using ambient traffic and moving force identification. *Structural Control and Health Monitoring*, 22:1396–1407, 2015.

[20] Aruz Petcherdchoo, Luis A Neves, and Dan M Frangopol. Optimizing lifetime condition and reliability of deteriorating structures with emphasis on bridges. *Journal of structural engineering*, 134(4):544–552

[21] Herbert E Rauch, CT Striebel, and F Tung. Maximum likelihood estimates of linear dynamic systems. *AIAA journal*, 3(8):1445–1450 0001–1452, 1965.

[22] Guido Roelfstra, Rade Hajdin, Bryan Adey, and Eugen Brühwiler. Condition evolution in bridge management systems and corrosion-induced deterioration. *Journal of Bridge Engineering*, 9(3):268–277

[23] Tariq Usman Saeed, Yu Qiao, Sikai Chen, Konstantina Gkritza, and Samuel Labi. Methodology for probabilistic modeling of highway bridge infrastructure condition:

Accounting for improvement effectiveness and incorporating random effects. *Journal of Infrastructure Systems*, 23(4):04017030

[24] Mauricio Sánchez-Silva, Dan M Frangopol, Jamie Padgett, and Mohamed Soliman. Maintenance and operation of infrastructure systems. *Journal of Structural Engineering*, 142(9):F4016004

[25] Dan Simon and Donald L Simon. Constrained kalman filtering via density function truncation for turbofan engine health estimation. *International Journal of Systems Science*, 41(2):159–171

[26] Jojok Widodo Soetjipto, Tri Joko Wahyu Adi, and Nadjadji Anwar. *Bridge Deterioration Prediction Model Based On Hybrid Markov-System Dynamic*, volume 138. EDP Sciences, 2017.

[27] Seung-Ie Yang, Dan M Frangopol, Yoriko Kawakami, and Luís C Neves. The use of lifetime functions in the optimization of interventions on existing bridges considering maintenance and failure costs. *Reliability Engineering System Safety*, 91(6):698–705

[28] Weili Zhang and Naiyu Wang. Bridge network maintenance prioritization under budget constraint. *Structural safety*, 67:96–104

A Appendix 1

A.1 Decision Making for Synthetic Interventions

The decision making for synthetic interventions is done based on if-then rules defined in Table 6. These rules have two inputs and one output, the inputs are the health condition and the priority index of the bridge, while the output is the type of the intervention. In order to limit the number of rules, the deterioration condition and the priority index are discretized into categories as shown in Figure 15. An example that demonstrates the use of this system is for a structural element that has a health condition 80 and priority 2.5, the applied intervention is h_2. Moreover, the health condition category V.D. refers to a very damaged state of which a replacement action is required. The replacement actions are not considered in this study, provided that this type of interventions results in changing the entire structural element.

Table 6: Table of synthetic interventions h_r applied for a given health condition and a priority index.

		Health Condition		
		Damaged	Good	Excellent
Priority	High	h_3	h_2	h_1
	Medium	h_3	h_2	h_0
	Low	h_2	h_1	h_0

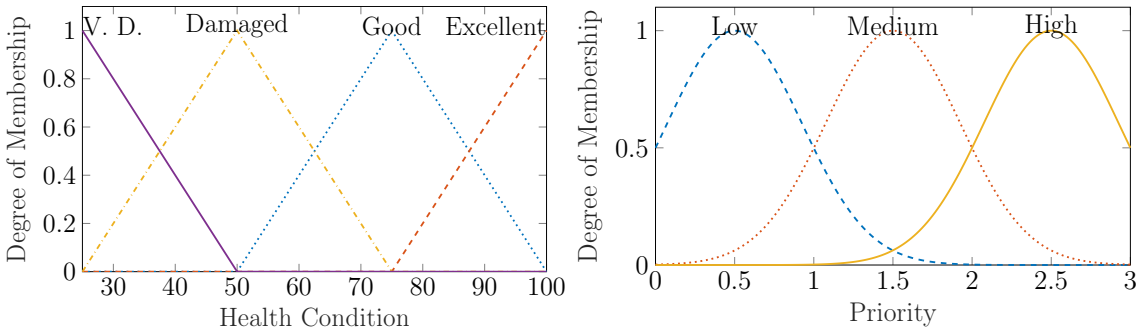

Figure 15: Categories for the health condition and the priority index.